Hyperfunction with normal inotropic state of the hypertrophied left ventricle

S. SASAYAMA, D. FRANKLIN, AND J. ROSS, JR.
Division of Cardiology, Department of Medicine, University of California, San Diego, School of Medicine and Scripps Clinic and Research Foundation, La Jolla, California 92037

SASAYAMA, S., D. FRANKLIN, AND J. ROSS, JR. *Hyperfunction with normal inotropic state of the hypertrophied left ventricle*. Am. J. Physiol. 232(4): H418-H425, 1977 or Am. J. Physiol.: Heart Circ. Physiol. 1(4): H418-H425, 1977. —Conscious dogs were instrumented with an inflatable cuff around the ascending aorta, a high-fidelity micromanometer in the left ventricle (LV), and pairs of ultrasonic crystals for measurements of LV wall thickness and internal LV diameter. Wall stress (WSt) and mean velocity of wall shortening (V_{CF}) were calculated. Mean force-velocity relations and WSt-diameter loops in single contractions were then analyzed over a range of matched systolic pressures during acute aortic constrictions both before and after induction of chronic hypertrophy by sustained aortic constriction. At normal LV systolic pressures and at each matched level of systolic LV pressure, wall shortening velocity was increased in the hypertrophied ventricle. However, force-velocity relations obtained by relating mean V_{CF} to mean WSt at various stress levels fell on the same relation as during control. The linear relation between LV diameter and pressure at the end of ventricular ejection was shifted to the left in the hypertrophied ventricle, indicating enhanced shortening. However, linear WSt-diameter relations at end-ejection were not different in control and hypertrophied hearts. These findings indicate that the ventricle hypertrophied by pressure overload exhibited hyperfunction as a pump but that its myocardium had a normal level of inotropic state.

pressure overload; afterloaded contractions; myocardial contractility; force-velocity relations; cardiac hypertrophy; cardiac dimensions; ultrasound; ventricular function

CARDIAC HYPERTROPHY PROVIDES a fundamental mechanism by which the heart can adapt to abnormal loading conditions, but whether or not hypertrophy is associated with depression of myocardial inotropic state has been controversial (21). We have developed an experimental model for chronic pressure overloading by aortic constriction in conscious dogs, which employs an ultrasonic technique for the simultaneous measurement of left ventricular wall thickness and diameter (23). This approach has permitted the serial assessment of left ventricular function over several weeks. Our previous study (23) indicated that the left ventricle responds to the pressure overload by initial dilatation with increased wall stress, followed by concentric hypertrophy, with a return to normal diastolic dimensions. This adaptive response was accompanied by a relation between peak wall stress and wall velocity in the steady state after hypertrophy which was not different from control, which we interpreted to represent a normal level of contractility, or inotropic state (19, 23).

The present study extends these observations to a further assessment of the contractility of the hypertrophied ventricle by comparing the dynamic responses to initial inflation of the cuff prior to hypertrophy with those occurring with reinflation of the cuff after release of chronic constriction, in the presence of hypertrophy. This approach has permitted a detailed analysis of force-velocity relations and wall stress-diameter loops during single contractions, as well as examination of length-tension relations at end-systole.

METHODS

Five mongrel dogs, weighing 19–36 kg (average 26.7 kg) underwent right thoracotomy in the fourth left intercostal space under sodium pentobarbital anesthesia (25 mg/kg, iv). As described previously, woven Dacron tubing was wrapped around the ascending aorta as a supporting sleeve, an inflatable rubber cuff was placed around the graft, tubing leading to the cuff was brought out between the ribs, and the injection bulb was implanted subcutaneously (23). A high-fidelity micromanometer (Konigsberg P-22) was inserted into the left ventricular chamber through a stab incision at the ventricular apex, and a catheter approximately 25 cm in length, 1.3 mm ID, 2.3 mm OD (S-54-HL; Norton Plastics, Akron, Ohio) was also positioned 1.5 cm into the left ventricle through the apex. One pair of ultrasonic crystals (5 MHz piezoelectric discs each 5 mm in diameter) was positioned at the anterior and posterior endocardial surfaces of the left ventricular cavity near the minor equator, and a second pair of crystals was placed across the left ventricular free wall (23). The internal crystal, 1.7 mm in diameter with a flat back and convex lens, was inserted blindly through a diagonal tract to a site just within the endocardium where it remained imbedded within the myocardium, lens facing outward (23); the flat disc-shaped external crystal, 3 mm in diameter, was attached to a 8 x 8 mm sheet and sutured to the epicardium at the point of shortest transit time to the internal crystal. Both crystals were fabricated in our laboratory. Potential errors due to crystal placement have been described previously (22, 23); there is little shear motion of the crystals during the cardiac cycle (11), but sometimes inward displacement of the

subendocardial crystal results in some underestimation of absolute wall thickness, or the crystals are not precisely opposed across the wall (23). The crystals usually can be accurately placed and they appear reliable for detecting relative acute and chronic changes in wall thickness (22). In only one dog in the present study was it possible to fix the heart in diastole shortly after an in vivo measurement; the last recorded end-diastolic wall thickness in vivo was within 1 mm of the intercrystal distance at post mortem (14 mm), and the measured wall thickness was 14 mm. In two dogs, the intercrystal distances at postmortem were 18 mm and 19 mm, which agreed with measured wall thicknesses of 18 and 19 mm (both hearts in rigor); one pair of crystals was slightly on the diagonal, the inner crystal 1 mm from the endocardium, and in the other pair the crystals were somewhat more diagonally placed, the inner crystal being 2 mm from the endocardium. In one dog, the intercrystal distance was 19 mm, the inner crystal being partly in the base of a papillary muscle, but the crystals were precisely opposed across the wall, and this measurement agreed with direct free wall thickness measurement. The fifth dog died over a holiday, and only the ventricular weight was obtained.

A pacing wire was attached to the right atrial appendage. All wires and the catheter were then exteriorized to the back of the animal, and the studies were initiated at least 10 days postoperatively when each dog had recovered completely.

Five dogs were selected for this analysis from among the group previously studied (23); they were selected because resting tracings could be closely matched for systolic pressure and heart rate, and satisfactory acute aortic constrictions of comparable degree were obtained on two occasions: under control conditions before hypertrophy, and 5–10 min following release of the cuff after the development of hypertrophy. The cuff was released at an average of 18 days (range 13–24 days). Spontaneous resting heart rates prior to pacing were not different before and 5–10 min after release of constriction (avg 82 and 80/min). Hypertrophy was present in all these dogs at postmortem examination, the left ventricle-to-body weight ratios averaging 5.78 g/kg (range 5.03 to 6.65 g/kg, average normal value 4.7 g/kg (17)), although two dogs were killed at 24 h after cuff release and three dogs at 7–10 days, so that some regression of hypertrophy had occurred in the latter (23).

Measurements were recorded while the animal was lying quietly awake on the floor. The cuff was inflated (Fig. 1) to elevate the peak systolic left ventricular pressure by about 50% above the control value. Atrial pacing of 100–120/min was performed during each constriction, the rates during the two constrictions being closely similar in each dog in order to avoid reflex effects on heart rate (Table 1). However, the contractions analyzed as the aorta was undergoing constriction were taken during the initial 5–10 seconds of constriction, prior to substantial reflex changes.

Measurements were recorded during each experiment on a Brush-Clevite forced-ink oscillograph and stored on magnetic tape for later playback and computations. The measured sonic transit time was calibrated in 1-μs.

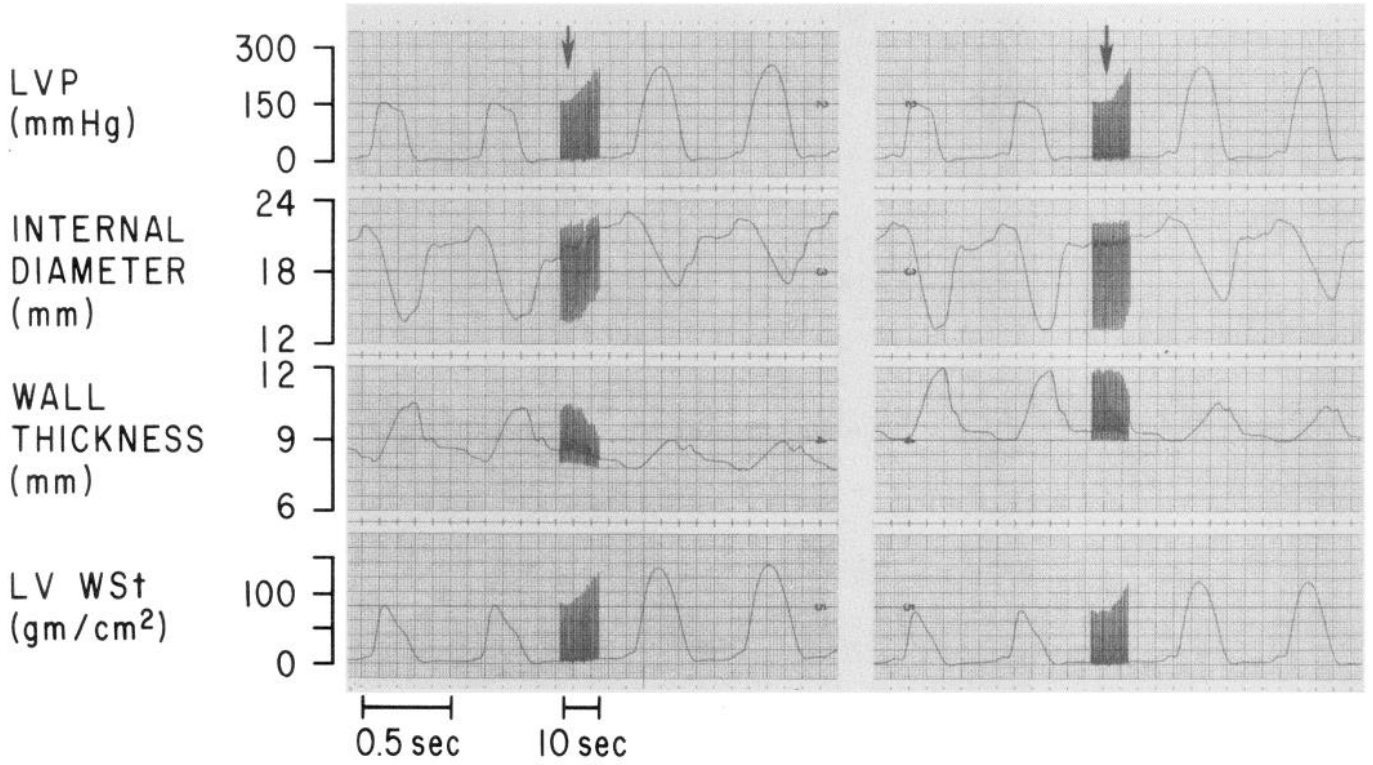

FIG. 1. Original tracings showing inflation of aortic cuff in control state (*left panel*). Following release of cuff after sustained aortic constriction for 15 days to produce hypertrophy, cuff was reinflated (*right panel*). From top to bottom are left ventricular pressure (LVP), internal LV diameter, LV wall thickness, and computed LV wall stress (WSt). Beginning of aortic constrictions is indicated by arrows.

TABLE 1. *Effect of acute aortic constriction on normal and hypertrophied ventricles*

	HR	LV Pressure, mmHg			LV Internal Diam, mm		LV Wall Thickness, mm		Wall Stress, gm/cm²				V_{CE}, circ/s
		ED	Peak	ES	ED	ES	ED	ES	ED	Peak	ES	Mean	
Control													
Before AAC	109±5	10.4±0.7	147.6±6.2	98.2±6.6	31.0±2.4	22.4±2.6	10.2±0.7	12.9±1.0	8.0±0.7	103.0±5.8	46.0±6.3	76.6±5.5	1.70±0.24
After AAC	112±5	16.8±2.8	208.8±3.1	136.2±6.3	31.8±2.6	25.1±2.9	10.0±0.7	12.0±0.9	13.6±2.3	139.0±8.8	74.6±8.3	113.7±8.5	1.12±0.20
P		<0.05	<0.001	<0.001	<0.05	<0.01	<0.05	NS	<0.05	<0.01	<0.01	<0.001	<0.001
Hypertrophied													
Before AAC	106±6	8.6±2.1	148.8±6.4	101±7.0	30.4±2.4	21.3±2.7	11.4±0.8	14.5±1.1	5.9±1.5	89.5±7.3	34.9±3.2	65.6±3.4	1.97±0.24
After AAC	108±6	14.0±2.4	208.2±3.4	130.6±7.9	30.7±2.5	22.6±3.0	11.3±0.8	14.0±1.0	10.0±2.1	116.7±9.9	49.4±5.6	91.1±5.8	1.51±0.24
P		<0.05	<0.001	<0.001	NS	<0.01	NS	NS	<0.05	<0.01	<0.05	<0.001	<0.001
P'		NS	NS	NS	NS	<0.05	<0.001	<0.01	NS	<0.05	NS	<0.05	<0.01
P''		NS	NS	NS	<0.05	<0.01	<0.001	<0.01	NS	<0.01	<0.05	<0.05	<0.05

Values are means ± SE, n = 5. Control, ventricles studied before production of hypertrophy by chronic aortic constriction. LV, left ventricular; ED, end-diastole; ES, end-systole; mean V_{CF}, mean normalized shortening rate; HR, heart rate; *P*, comparison before and after acute aortic constriction (AAC); *P'*, comparison before acute aortic constriction (AAC) of control to hypertrophied ventricles; *P''*, comparison at the end of acute aortic constriction (AAC) of control and hypertrophied ventricles.

increments against a standard signal of precisely known duration derived from a stable crystal-controlled oscillator (1.000 MHz); other details of the ultrasonic technique have been described elsewhere (30). The micromanometer, which afforded high-fidelity recordings of left ventricular end-diastolic and systolic pressures during aortic constrictions, was calibrated by adjusting its output to match the pressure measured through the fluid-filled catheter (23). Each micromanometer gauge was characterized prior to implantation. The temperature sensitivity was verified to be less than 1 mmHg/°C over the range of 32–42°C. The pressure sensitivity was established and the zero pressure electrical output signal was determined using the excitation voltage (5.46 V, regulated supply) which was employed during all experiments. The resistive compensation network selected during calibration was used in all experiments. End-diastolic pressure was measured directly via the catheter using an externally connected Statham P23Db transducer, thus establishing a zero base-line calibration to correct for zero drift of the micromanometer during most experiments. (In two of the five dogs the implanted catheter ultimately clotted, and the final calibrations were established using retrograde left ventricular catheterization with a Millar catheter-tip pressure gauge). Finally, the gauge was excised and the original calibration procedures were repeated in vitro. Thus, although most of the micromanometers offset gradually to some degree in both zero level and sensitivity during the long implantation, the multiple calibration procedures employed in these experiments provided direct calibration points so that the electrical signal from the micromanometer could be accurately related to instantaneous intraventricular pressure.

The computation of estimated instantaneous left ventricular wall stress (WSt), expressed as $WSt = P \cdot D/4 \cdot WTh$ (where P is pressure, D is internal diameter, and WTh is wall thickness), was obtained by an analog multiplier and a divider. The mean value of WSt was measured by planimetric integration of the wall stress wave form during ventricular ejection. The pressure signal, or wall stress signal, was fed into a storage oscilloscope on the *y*-axis and the diameter signal on the *x*-axis to produce pressure-diameter (P-D) loops or WSt-D loops during individual cardiac cycles. The P-D and WSt-D relationships athe end of ejection were analyzed and averaged on photographs (see Fig. 4) of several superimposed loops before and after pressure elevation in control recordings, and also during the second inflation of the cuff after hypertrophy had occurred; these points at the end of ejection appeared to form a linear relation in a series of beats obtained during a single pressure elevation, a finding previously described in a different series of normal, conscious dogs subjected to phenylephrine infusions (13). In each dog, data points were averaged before and after full aortic constriction (Fig. 2). The average relations were obtained by analysis of the straight line connecting the averages of these two points. The slopes and intercepts of these relations were then compared between normal and hypertrophied ventricles (Fig. 5).

The mean velocity of circumferential fiber shortening (mean V_{CF}) was obtained by dividing stroke excursion of D (from end-diastole to the end of shortening) by the ejection period (estimated as the time from peak dP/dt to the nadir of the diameter tracing, as described previously (23)). Mean V_{CF}, normalized to per unit end-diastolic dimension by dividing by end-diastolic diameter (usually expressed as circumferences per second (9)), was related to peak pressure and to peak and mean WSt in each cardiac cycle before and after pressure elevations to obtain stress-velocity relations. The average pressure-velocity and stress-velocity relations were analyzed as the straight line connecting the average of these two points in each dog (Fig. 2), and for each group, before and after hypertrophy (Fig. 3). Mean V_{CF} has previously been used in man (9) and experimental animals (18, 20, 21) as a measure of contractility in the basal resting state, and its sensitivity to acute changes in afterload has been documented (14).

The values of wall stress reported in the tables and Figs. 3–5 were obtained directly from the tracings made from the analog computations of wall stress, using hemodynamic and dimension data from the original tapes. In addition, a somewhat more complex thick-walled equation for wall stress (3) was compared with the above simplified equation: $WSt = PR^2_i/(R_o^2 - R^2_i)$. For application of the latter equation, pressure and diameter relations were taken directly from pressure and length tracings, R_o and R_i were determined at the midpoint between end-diastole and end-systole. Use of the more complex equation yielded wall stress-velocity relations

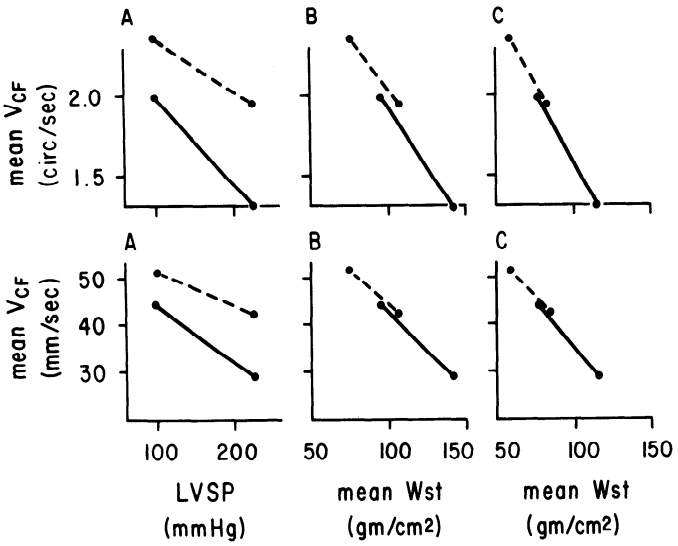

FIG. 2. Alternative methods of calculating relations between pressure, wall stress (WSt), and velocity of shortening (V_{CF}) in a single experimental animal. Dashed lines, hypertrophy; solid lines, control state. Upper 3 panels (*A*, *B*, and *C*) show mean V_{CF} values normalized for end-diastolic circumference (circ); in lower 3 panels V_{CF} is not normalized. Panels labeled *A* show relations of mean V_{CF} to peak left ventricular systolic pressure (LVSP), those labeled *B* show mean V_{CF} related to mean WSt calculated by a simplified equation, and those labeled *C* show use of a more complex thick-walled equation for WSt (see text). In this example, representative of 2 dogs exhibiting detectable differences, only slightly better overlap between V_{CF}-wall stress relations before and after hypertrophy are noted with the more complex equation.

for control and hypertrophied hearts which were not detectably different, having slopes of -0.021 ± 0.004 (SE) and -0.023 ± 0.004, and intercepts of 2.99 ± 0.34 and 3.16 ± 0.35 for control and hypertrophied hearts, respectively. For wall-stress–diameter relations at end-systole, the slopes averaged 10.5 ± 0.9 and 10.6 ± 0.9, and the intercepts averaged -204 ± 37 and -201 ± 31 for control and hypertrophied hearts, respectively. A representative example comparing such calculations in *dog A* is shown in Fig. 2. Although slightly improved coincidence of the relations was noted in two dogs, since these calculations did not alter the conclusions significantly compared with data obtained using the simpler equation in the analog computer, the latter are reported in Table 2 and in the figures. In addition, the data were calculated using values for V_{CF} that were not normalized for end-diastolic circumferences. This approach did not produce any perceptible difference in the interpretation of the data; a representative example of this calculation is shown in Fig. 2.

A paired *t*-test was used for all statistical analyses.

RESULTS

In Fig. 1, representative tracings are reproduced showing responses to acute pressure overload in the control state and after the development of left ventricular (LV) hypertrophy in the same dog. The averaged data derived from hemodynamic measurements and dimensions are summarized in Table 1.

With acute aortic constriction in the control state, peak LV systolic pressure was elevated from an average of 148 to 209 mmHg associated with an increase in LVEDP from 10 to 19 mmHg. LVEDD was augmented by 3% over the control value of 31.0 mm with an increase in LVESD by 12% from 22.4 mm. WSt was elevated at end-diastole and it also increased at end-systole; peak and mean WSt were augmented from 103 to 139, and from 76.6 to 113 g/cm^2, respectively. The mean V_{CF} was reduced by 34% below the control value of 1.70 circ/s.

Upon the release of chronic aortic constriction, measurements were made in the resting state at peak systolic pressures and heart rates closely matched to the control values before aortic constriction (Table 1). EDP and EDD were slightly but not significantly decreased compared to control values. ESD was 5% smaller than control, but EDWTh and ESWTh were significantly increased by 12% over control values. Consequently, peak and mean WSt were significantly decreased below control by 11% and by 24%, respectively, despite equivalent levels of peak LV systolic pressure, and mean V_{CF} was augmented by 16% (Table 1).

The aortic cuff was then reinflated to elevate the LV peak systolic pressure to the same level as during the initial aortic constriction, prior to the development of hypertrophy. At the second constriction, the same directional changes were observed, but the increase of EDD was only 1% and augmentation of ESD was 6%, reflecting less marked reduction in the stroke excursion. Figure 3, *left panel*, illustrates the effects of acute pressure loading on mean V_{CF} in the control state (solid line) and after hypertrophy (dashed line). The pressure-velocity relation was clearly displaced upward, mean V_{CF} being significantly elevated at the same pressure levels after hypertrophy (Table 1). When mean WSt was related to mean V_{CF} after hypertrophy, mean WSt was significantly lower and mean V_{CF} was higher both before and after acute aortic constriction (Table 1); however, the force-velocity relation of hypertrophied ventricles fell on

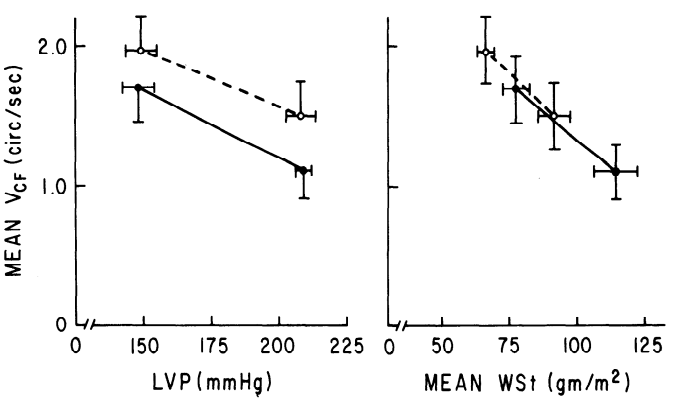

FIG. 3. Relations between mean internal diameter shortening rate normalized by end-diastolic internal diameter (mean V_{CF}, expressed as circumferences or muscle lengths per second) and left ventricular pressure (LVP) (*left*) or mean wall stress (WSt) (*right*) in control state (solid lines) and after hypertrophy (dashed lines). Circles indicate means and brackets indicate SE at beginning and end of pressure elevations. Mean V_{CF} was significantly elevated at each pressure level after hypertrophy. However, when mean V_{CF} was related to mean wall stress, the force-velocity relation of hypertrophied ventricles fell on that of control state.

the same relation as in the control state (Fig. 3, *right panel*). The slopes and the intercepts of these straight lines could not be distinguished statistically (Fig. 3 and Table 2).

Figure 4, *left panels*, demonstrates examples of superimposed P-D loops obtained in one animal during the early course of acute pressure loading in the normal (*upper left panel*) and hypertrophied state (*lower left panel*). Corresponding WSt-D loops obtained by analogue computation of WSt in the same experiment are shown in Fig. 4, *right panels*. Under resting conditions, the P-D loops exhibit a parallelogram with varying degrees of inclination toward the left, and with aortic constriction their configuration becomes more rounded at the peak because of altered configuration of the LV pressure tracing as well as to less shortening during ejection. However, the points relating length to pressure at the end of active shortening in each series of beats appear to form an approximately linear relation. This relation was shifted to the left after hypertrophy due to somewhat reduced end-diastolic dimensions and augmented shortening at each pressure level. When the WSt-D relation was obtained, the shape of the loops was generally different from P-D loops in that the stress decreased during ejection relatively more than the pressure, as chamber size decreased while the wall thickness increased. After hypertrophy, stresses were lower with somewhat decreased end-systolic lengths (Fig. 4, *right panels*).

The relations between LVP, WSt, and internal diameter at the end of shortening (ESID) were analyzed before and after acute aortic constrictions. The relation between LVP and ESID was clearly displaced upward and to the left after hypertrophy (Fig. 5, *left panel*), LV diameters at end-systole being significantly less at closely similar end-systolic pressures after hypertrophy compared to control (Table 1). ESWSt values were significantly less after hypertrophy at the same pressure levels, as a consequence of the smaller end-systolic chamber size together with increased wall thickness due to hypertrophy (Fig. 5, *right panel*). Therefore, the straight lines connecting end-systolic points in WSt-diameter relations of control and hypertrophied hearts were statistically indistinguishable from each other in terms of their slopes and intercepts (Fig. 5, Table 2).

TABLE 2. *Relations between wall stress-diameter and wall stress-velocity in dogs before and after left ventricular hypertrophy*

Condition	WSt-D Relation		WSt-V_{CF} Relation	
	Slope	Intercept	Slope	Intercept
Dog W				
Control	15.3	−360	−0.020	2.80
Hypertrophy	16.4	−368	−0.016	2.49
Dog G				
Control	11.2	−274	−0.013	2.02
Hypertrophy	11.3	−278	−0.018	2.45
Dog P				
Control	14.2	−251	−0.028	4.05
Hypertrophy	14.7	−258	−0.031	4.36
Dog A				
Control	12.9	−152	−0.015	3.44
Hypertrophy	15.4	−187	−0.013	3.33
Dog T				
Control	9.3	−154	−0.014	3.05
Hypertrophy	9.5	−158	−0.019	3.38
Average				
Control	12.6 ± 1.1	−238 ± 39	−0.018 ± 0.003	3.07 ± 0.34
Hypertrophy	13.5 ± 1.3	−249 ± 37	−0.019 ± 0.003	3.20 ± 0.35

Control, studies before chronic aortic constriction to produce hypertrophy; hypertrophy, studies in same dogs after chronic aortic constriction. WSt-D relation, line connecting wall stress (WSt) and diameter (D) points at the end of active shortening before and after acute aortic constrictions. WSt-V_{CF} relations, line connecting mean wall stress-mean V_{CF} points. ±, SE. Slopes and intercepts before and after hypertrophy cannot be separated statistically.

DISCUSSION

Although left ventricular function has been assessed in response to acute interventions in conscious, intact animals (8, 14, 17, 21), little is known about the chronic changes in the contraction mechanics of the intact left ventricle that occur in response to sustained pressure overload, as reviewed elsewhere (21, 23). Spann et al. (26) documented depressed isometric length-tension curves in isolated muscle strips taken from the right ventricles of cats after 6 wk of pulmonary artery constriction and concluded that depressed function was a fundamental characteristic of myocardium hypertrophied by pressure overload; Spann's conclusion of depressed inotropic state in pressure-induced hypertrophy, on the basis of force-velocity analysis of isolated cat papillary muscles, was supported by similar results in subsequent experiments (1, 2, 5, 10), although Bing et al. (2) did not observe depressed tension development. However, Williams and Potter (31) recently carried out similar experiments to those of Spann et al. and found normal contractile function of isolated muscles obtained after longer periods of pulmonary artery constriction. They emphasized the need for defining the temporal relationships between inotropic state level and the degree and duration of constriction (31). Fisher and Kavaler (7) measured the isometric force in right ventricular papillary muscles in situ in pulmonary artery-banded dogs and found a normal rate of rise of force in the hypertrophied muscles. They postulated that the depressed function shown in Spann's experiments might be due to greater distance for diffusion between the surface and the center of the isolated muscles in the in vitro setting (7). In a clinical study, Mason et al. (15) utilized the relationship between isovolumic systolic pressure and dP/dt to obtain "Vmax," and reported that cardiac inotropic state under basal conditions was depressed in the hypertrophied, nonfailing heart. Levine et al. (12) on the other hand, with calculation of "contractile element velocity" from isovolumic phase pressure tracings described normal indices of contractility in 8 of 12 subjects with aortic stenosis who had no evidence of heart failure. Simon et al. (24) also calculated pressure-velocity relationships throughout the isovolumic phase of systole in patients with aortic stenosis and failed to find depressed function in patients with aortic stenosis and pressure gradients below 50 mmHg.

In the present study, the shortening characteristics of the left ventricular wall during ejection were assessed by the mean velocity of circumferential shortening at

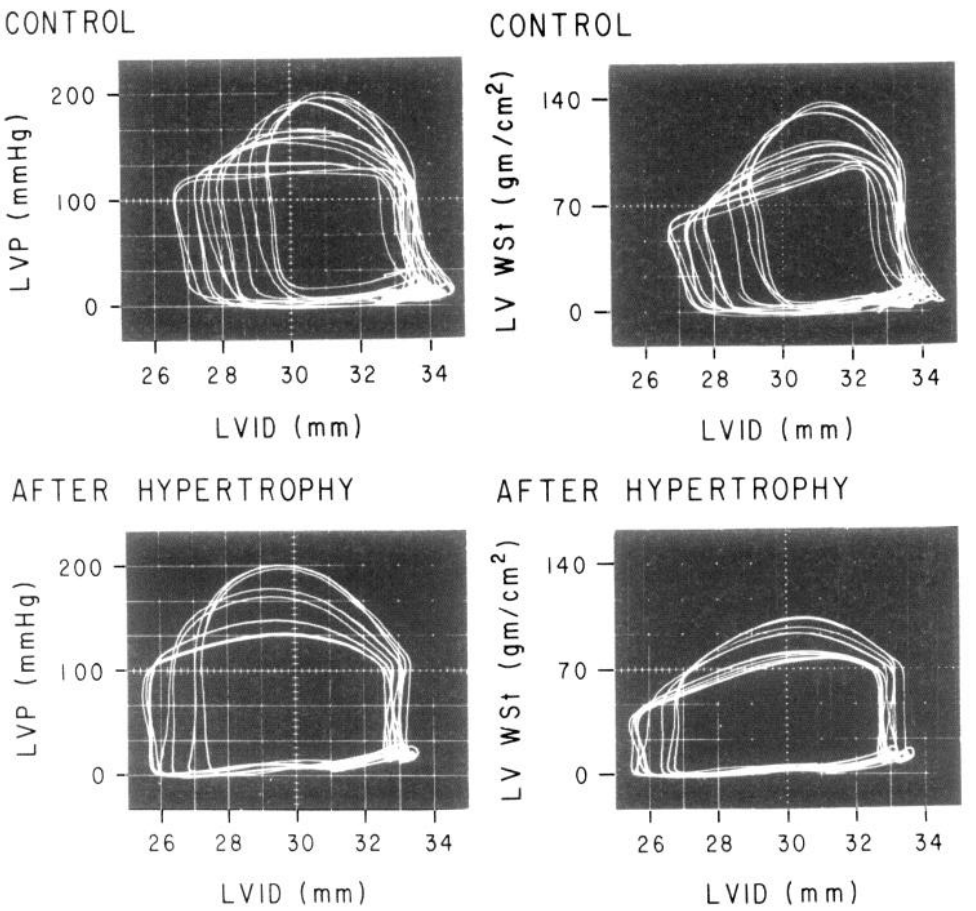

FIG. 4. Superimposed pressure-diameter (*left*) and wall stress-diameter loops (*right*) in resting state and for several cardiac cycles during aortic cuff inflation. Upper loops were obtained during control state prior to hypertrophy and lower loops were recorded during reconstriction of aorta after development of hypertrophy in the same dog. LVP, ventricular pressure; LV WSt, left ventricular wall stress; LVID, left ventricular internal diameter.

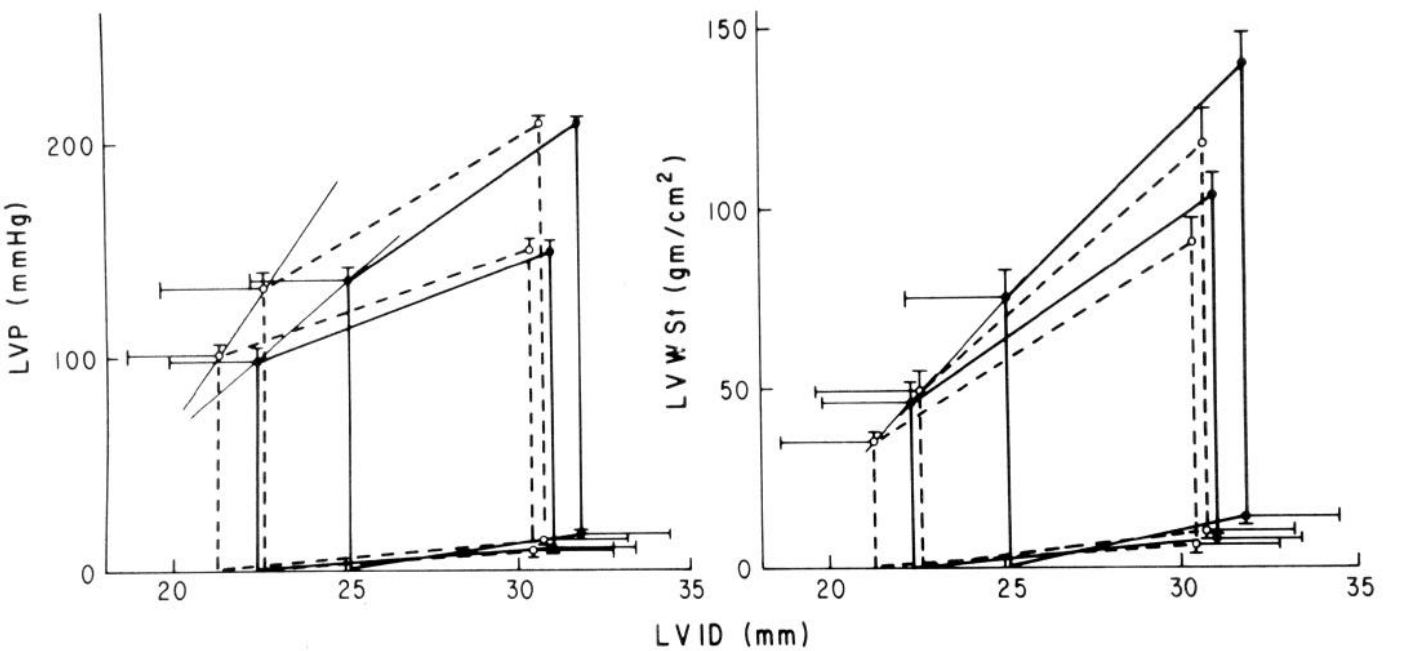

FIG. 5. Representation of averaged pressure-diameter (*left*) and wall stress-diameter loops (*right*) before and after inflation of aortic cuff in control state (solid lines) and after development of hypertrophy (dotted lines). Representative loops were averaged in all dogs at beginning and at end of cuff inflation. Peak systolic pressures were matched before and during aortic constriction. Note that wall stress-diameter relation at end-ejection of hypertrophied ventricle was not different from that of control. (Abbreviations as in Fig. 3.) $n = 5$. Brackets indicate SE.

the minor equator corrected for end-diastolic dimension, and by the relation between wall stress and ventricular diameter at end-ejection. The relationship between normalized wall shortening velocity and the mean wall stress can be used as an index of basal inotropic state per unit of muscle under normal resting conditions (20) and permits the comparison of a basal level of contractility in normal and hypertrophied ventricles after adaptation is accomplished by an increase in muscle mass (19). Wall stress was estimated by analog computation using a spherical model. Although wall stress is better approximated by thick-walled ellipsoidal model (21), a measurement of the ventricular long axis was not available, and this simplified estimation is a convenient and useful approximation for assessing relative changes in wall stress in the same heart before and after an intervention. Moreover, as discussed earlier, use of a more complex equation did not change the interpretation of our results. The ultrasound technique employed appears highly suitable for such calculations in conscious animals by providing continuous recordings of instantaneous dimensions and direct display of phasic patterns of computed wall stress and length-tension relationships.

A single measurement of V_{CF} does not necessarily reflect inotropic state under nonbasal conditions because it is affected by acute afterload changes (14), and therefore an induced range of afterloads was studied. The pressure-velocity relation so obtained indicated significant hyperfunction in the hypertrophied ventricle at each matched pressure level. Also, hyperfunction of the hypertrophied ventricle was evident under basal conditions, mean V_{CF} being augmented over control because of a concomitant decrease in mean wall stress, related to increased wall thickness. However, when the relation between mean WSt and mean V_{CF} was studied over a range of WSt values, the hypertrophied ventricle showed no detectable difference from control; thus, there was no evidence of altered inotropic state in the concentrically hypertrophied ventricle subjected to a sustained pressure overload.

We also examined the relation between ventricular diameter and wall stress at the end of ejection as a further measure of the level of inotropic state. The length-tension relation of cat papillary muscles contracting isometrically tends to be similar to that obtained with variably afterloaded isotonic contractions (25). Thus, the muscle shortens to the same point on the tension curve under a given load, independent of initial resting muscle length; interventions that change the level of inotropic state cause a shift in the active tension curve without a change in resting tension (25). In the length-tension diagrams described in closed-chest *sedated dogs subjected to variable afterloading* (29), isolated heart preparations contracting isotonically (4) or isobarically (16), and in pressure-diameter loops recorded during serial changes following phenylephrine injection (13), the points at the end of shortening were shown to be on a straight line with high correlation coefficients. Pressure-volume data points near end-ejection obtained in the denervated heart with arterial pressure fixed at different levels and constant cardiac output showed a linear correlation between volume and pressure near end-ejection (28), and other acute studies in isolated hearts showed that the time-varying ratio of pressure to volume was independent of end-diastolic volume and arterial pressure but was affected by acute changes in inotropic state (27). Thus, although some discrepancies between isometric and isotonic length-tension relationships may be encountered (29), several studies in the whole heart have indicated that analysis of length-tension or pressure-volume relationship at the end of ejection generally approximate the isovolumic length-tension relation (4, 6, 13, 16, 29). Therefore, we have employed it in the present study to provide an additional measure of the level of inotropic state and, again, the hypertrophied ventricle showed no detectable change from the control state when wall stress was employed.

These findings support our previous studies obtained in a larger number of animals under more variable, resting conditions (23). That study also provided evidence that acute reflex or neurohumoral changes after release of aortic constriction did not play a significant role in the observed responses, since contractile responses remained closely similar under basal conditions 24 hours after the release (23). The more detailed analysis in the present study has documented augmented pumping capability of the concentrically hypertrophied ventricle by demonstrating shifts of the pressure-diameter relation at end-ejection and the pressure-velocity relation. The lack of change of the stress-diameter relation at end-ejection, together with the demonstration that the entire force-velocity relation appeared unchanged, further supports the conclusion that inotropic state was normal. This adaptation to chronic pressure overload, in which the end-diastolic dimension is not enlarged, differs from that of the left ventricle subjected to marked chronic volume overloading, in which eccentric hypertrophy occurs. In that setting, progressive dilatation and maximum use of preload permits enhancement of cardiac stroke volume but with normal performance of each unit length of circumference and, again, a normal level of inotropic state (18, 19). Differences between our studies and previous investigations on the inotropic state of muscle hypertrophied by chronic pressure overload may relate in part to differences in the duration and the severity of the imposed load.

This project was supported by National Institutes of Health, Research Grant HL-12373, awarded by the National Heart, Lung, and Blood Institute.

Address reprint requests to J. Ross, Jr., Director, Division of Cardiology, Department of Medicine, M-013, University of California, San Diego, La Jolla, California 92093

Received for publication 20 May 1976

REFERENCES

1. BASSETT, A. L., AND H. GELBAND. Chronic partial occlusion of the pulmonary artery in cats. Change in ventricular action potential during early hypertrophy. *Circulation Res.* 32: 15–26, 1973.

2. BING, O. H. L., S. MATSUSHITA, B. C. FANBURG, AND H. J. LEVINE. Mechanical properties of rat cardiac muscle during experimentatl hypertrophy. *Circulation Res.* 28: 234–245, 1971.
3. BURNS, J. W., J. W. COVELL, R. MYERS, AND J. ROSS, JR. Comparison of directly measured left ventricular wall stress and stress calculated from geometric reference figures. *Circulation Res.* 28: 611–621, 1971.
4. BURNS, J. W., J. W. COVELL, AND J. ROSS, JR. Mechanics of isotonic left ventricular contractions. *Am. J. Physiol.* 224: 725–732, 1973.
5. COOPER, G. IV, R. M. SATAVA, C. E. HARRISON, AND H. N. COLEMAN III. Mechanism for the abnormal energetics of pressure-induced hypertrophy of cat myocardium. *Circulation Res.* 33: 213–223, 1973.
6. CROSS, C. E., P. A. RIEBEN, AND P. F. SALISBURY. Influence of coronary perfusion and myocardial edema on pressure-volume diagram of left ventricle. *Am. J. Physiol.* 201: 102–108, 1961.
7. FISHER, V. J., AND F. KAVALER. Maximal force development by hypertrophied right ventricular papillary muscles remaining in situ. In: *Cardiac Hypertrophy,* edited by N. R. Alpert. New York: Academic, 1971, p. 371–385.
8. VATNER, S. F., AND E. BRAUNWALD. Cardiovascular control mechanisms in the conscious state. *New Engl. J. Med.* 293: 970–976, 1975.
9. KARLINER, J. S., J. H. GAULT, D. L. ECKBERG, C. B. MULLINS, AND J. ROSS, JR. Mean velocity of fiber shortening: a simplified measure of left ventricular myocardial contractility. *Circulation* 44: 323–333, 1971.
10. KAUFMAN, R. L., H. HOMBURGER, AND H. WIRTH. Disorder in excitation-contraction coupling of cardiac muscle from cats with experimentally produced ventricular hypertrophy. *Circulation Res.* 28: 346–357, 1971.
11. KEMPER, W. S., S. SASAYAMA, D. MCKOWN, AND D. FRANKLIN. Ultrasonic triangulation technique for measurement of ventricular wall thickness and myocardial shear in vivo. *Proc. ACEMB, 28th, 1975* p. 451.
12. LEVINE, H. J., K. M. MCINTYRE, J. G. LIPANA, AND O. H. L. BING. Force-velocity relations in failing and nonfailing hearts of subjects with aortic stenosis. *Am. J. Med. Sci.* 259: 79–89, 1970.
13. MAHLER, F., J. W. COVELL, AND J. ROSS, JR. Systolic pressure-diameter relations in the normal conscious dog. *Cardiovascular Res.* 9: 447–455, 1975.
14. MAHLER, F., J. ROSS, JR., R. A. O'ROURKE, AND J. W. COVELL. Effects of changes in preload, afterload, and inotropic state on ejection and isovolumic phase measures of contractility in the conscious dog. *Am. J. Cardiol.* 35: 626–634, 1975.
15. MASON, D. T., J. F. SPANN, JR., R. ZELIS, AND E. A. AMSTERDAM. Comparison of the contractile state of the normal, hypertrophied, and failing heart in man. In: *Cardiac Hypertrophy,* edited by N. R. Alpert. New York: Academic, 1971, p. 433–444.
16. MONROE, R. G., AND G. N. FRENCH. Left ventricular pressure-volume relationships and myocardial oxygen consumption in the isolated heart. *Circulation Res.* 9: 362–374, 1961.
17. O'ROURKE, R. A., B. PEGRAM, AND V. S. BISHOP. Variable effect of angiotensin infusion on left ventricular function. *Cardiovascular Res.* 6: 240–247, 1972.
18. ROSS, J., JR. Adaptation of the left ventricle to chronic volume overload. *Circulation Res.* 35, Suppl. II: 64–70, 1974.
19. ROSS, J., JR. Afterload mismatch and preload preserve: a conceptual framework for the analysis of ventricular function. *Progr. Cardiovascular Dis.* 18: 255–264, 1976.
20. ROSS, J., JR., AND K. L. PETERSON. *On the Assessment of Cardiac Inotropic State.* [An editorial.] *Circulation* 47: 435–438, 1973.
21. ROSS, J., JR., AND B. E. SOBEL. Regulation of cardiac contraction. *Ann. Rev. Physiol.* 34: 47–90, 1972.
22. SASAYAMA, S., D. FRANKLIN, J. ROSS, JR., W. S. KEMPER, AND D. MCKOWN. Dynamic changes in left ventricular wall thickness and their use for analyzing cardiac function in the conscious dog. *Am. J. Cardiol.* 38: 870–879, 1976.
23. SASAYAMA, S., J. ROSS, JR., D. FRANKLIN, C. M. BLOOR, S. BISHOP, AND R. B. DILLEY. Adaptations of the left ventricle to chronic pressure overload. *Circulation Res.* 38: 172–178, 1976.
24. SIMON, H., H. P. KRAYENBUEHL, W. RUTISHAUSER, AND B. O. PRETER. The contractile state of the hypertrophied left ventricular myocardium in aortic stenosis. *Am. Heart J.* 79: 587–602, 1970.
25. SONNENBLICK, E. H. Instantaneous force-velocity-length determinants in the contraction of heart muscle. *Circulation Res.* 16: 441–451, 1965.
26. SPANN, J. F., R. A. BUCCINO, E. H. SONNENBLICK, AND E. BRAUNWALD. Contractile state of cardiac muscle obtained from cats with experimentally produced ventricular hypertrophy and heart failure. *Circulation Res.* 21: 341–354, 1967.
27. SUGA, H., AND K. SAGAWA. Instantaneous pressure-volume relationships and their ratio in the excised, supported canine left ventricle. *Circulation Res.* 35: 117–126, 1974.
28. SUGA, H., K. SAGAWA, AND A. A. SHOUKAS. Load independence of the instantaneous pressure-volume ratio of the canine left ventricle and effects of epinephrine and heart rate on the ratio. *Circulation Res.* 32: 314–322, 1973.
29. TAYLOR, R. R., J. W. COVELL, AND J. ROSS, JR. Volume-tension diagrams of ejecting and isovolumic contractions in left ventricle. *Am. J. Physiol.* 216: 1097–1102, 1969.
30. THEROUX, P., D. FRANKLIN, J. ROSS, JR., AND W. S. KEMPER. Regional myocardial function during acute coronary artery occlusion and its modification by pharmacologic agents in the dog. *Circulation Res.* 35: 896–908, 1974.
31. WILLIAMS, J. F., AND R. D. POTTER. Normal contractile state of hypertrophied myocardium after pulmonary artery constriction in the cat. *J. Clin. Invest.* 54: 1266–1272, 1974.